



University of Colorado
Denver



beam-driven **surface wave modes**
in
hollow **crystals**
“fiber accelerator”

Aakash Sahai

Prof. Toshiki Tajima

aakash.sahai@gmail.com

Bulk plasma acceleration

- plasma blowout regime - severe limitations **although** been very successfully demonstrated
- e⁻-beam acc. → **coupled** longitudinal & transverse wakes & **plasma-ion** problems
- e⁺-beam acc. → **overcome** ion-defocusing / phase-mix e⁻
- Hollow-channel → channel-wall current / fringe-fields

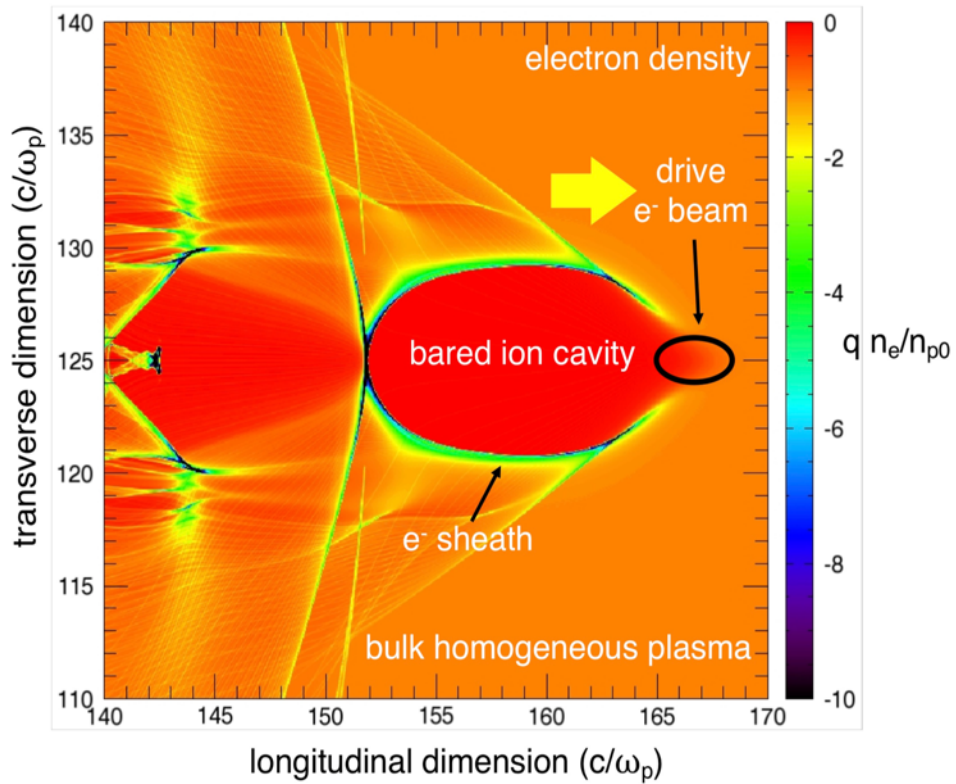
Crystal hollow nanotube modes

- Surface plasmon polariton (short time-scales), surface phonon polariton mode (longer time-scales)
- SW-CNT, MW-CNT modes
- Beam-driven modes in the hollow region – plasmon-polariton vs phonon-polariton modes
- **3D PIC** results of **driver independence** → occurs for e⁺ / e⁻ drive beams

Ongoing Work

- Acceleration / Focusing field → **decoupled – no ions**
- Driver affect → **head-erosion / etching – diff from bulk Plasma**
- Beam-loading → positron / electron beam in “crunch-in” wakefields

Bulk plasma Blowout regime – fundamental limitations



- Degradation of accelerated beam qualities its emittance, energy spread etc.
- strong coupling between longitudinal and transverse wakefields – **radiation loss**
- particles scattering off background ions (heavier ion plasma) – **sec. ioniz. & dark current**
- field degradation due to ion motion & ion modes (lighter ion plasma)
- positron and bared ions in the blowout region both being positively charged

Hollow “fiber” accelerator - 1983



Tajima, T., *Laser accelerators for ultra-high energies*, *Proceedings, 12th International Conference on High-Energy Accelerators*, pp. 470-472, C830811, HEACC 1983: Fermilab, Batavia, August 11-16, 1983

LASER ACCELERATOR FOR ULTRA-HIGH ENERGIES

T. Tajima

Department of Physics and Institute for Fusion Studies
 University of Texas, Austin, Texas 78712

Abstract

It is shown that under appropriate conditions the laser electromagnetic wave is trapped in a plasma fiber and is capable of exciting a beat plasma wave with a flat phase front propagating with the speed of light c (or any desired speed). In an important special case where the fiber contains vacuum inside it is still possible to have a wave whose phase velocity is up to c in the direction of the particle propagation with a plasma slow wave structure or in curved geometry. While the parallel component of the laser field is used for acceleration, the perpendicular component is either cancelled by the imposed static magnetic field force or used directly to contain particles. In the latter way it does not seem impossible to reach multi-peta electronvolts ($> 10^{15}$ eV) for protons. As examples of applications, I propose (i) direct method of collective excitations of quark-gluon systems; (ii) microscope for quark-gluon systems; (iii) method of direct interaction with spin or chiral structure of matter; and (iv) possible lasing by quark excitation.

I. Introduction

The laser beat-wave accelerator scheme¹ is capable of creating a coherent large longitudinal electric field $E_L = mc\omega_p/e$ of the order of 1 GeV/cm. Applying this scheme to an ultra-high energy accelerator has been considered.^{2,3,4} Two of the difficulties associated with the original scheme identified are: (i) the longitudinal phase mismatch between the plasma wave and the particles; (ii) the tendency of laser light to spread in the transverse direction. It is crucial to overcome these

One important case of the plasma fiber accelerator is a circular or race-track accelerator for protons utilizing the laser electric field to bend their orbit in order to contain particles within a manageable size. If such a scheme proves feasible, proton energies of multi-petaelectronvolts are not out of scope. We touch upon this in Sec. III.

In the last Section applications of such an accelerator, if it is ever successfully built, are suggested. A novel aspect in these is to directly couple the macroscopic beam structure with collective modes of the microscopic subnuclear structure.

II. Plasma Fiber Accelerator⁶

A way to match the phase of the accelerating field with high energy particles is to inject particles oblique to the electric field direction [see Fig. 1(a)]. In order to phase-lock, the angle θ between the particle momentum and the electric field is given by

$$\cos \theta = \left(1 - \frac{\omega_p^2}{\omega_0^2}\right)^{1/2}. \quad (2)$$

Although we match the parallel phase, we have now introduced an extraneous perpendicular acceleration, which bends the particle orbit (perhaps undesirably). To correct this situation, it was proposed⁷ that a static vertical magnetic field is imposed. The magnetic field is such that

$$\frac{B}{E} = \sin \theta = \frac{\omega_p}{\omega_0}, \quad (3)$$

for relativistic particles where B is out of the board in Fig. 1(c).

- hollow tube in plasma
- guide & self-focus high-intensity laser pulse
- phase velocity close to speed of light (low on-axis density)
- low ion concentration – on-axis minimize acc. beam plasma-ion interaction

Hollow “fiber” acc. – further work



laser-pulse driven

Laser wakefield acceleration and optical guiding in a hollow plasma channel

T. C. Chiou, T. Katsouleas, C. Decker, W. B. Mori, J. S. Wurtele, G. Shvets, and J. J. Su

Citation: *Physics of Plasmas* (1994-present) **2**, 310 (1995); doi: 10.1063/1.871107

channel. The electromagnetic fringe fields of the wake extend to the center of the channel, enabling focusing and acceleration of particles down the axis. This scheme differs from conventional hollow fiber accelerators, so that the wake fields arise from surface currents at the channel edge rather than density bunching at the channel axis.

Control of focusing forces and emittances in plasma-based accelerators using near-hollow plasma channels

PHYSICS OF PLASMAS **20**, 080701 (2013)

C. B. Schroeder, E. Esarey, C. Benedetti, and W. P. Leemans
Lawrence Berkeley National Laboratory, Berkeley, California 94720, USA

The wake excited in such a channel will consist of an electromagnetic wake owing to surface currents driven in the channel walls and a wake owing to the background ions in the channel. In the limit $k_c^2 \ll k_w^2$, the accelerating field in



University of Colorado
Denver



Hollow “fiber” acc. – beam-driven

electron-beam driven

VOLUME 81, NUMBER 16

PHYSICAL REVIEW LETTERS

19 OCTOBER 1998

High Beam Quality and Efficiency in Plasma-Based Accelerators

T. C. Chiou and T. Katsouleas

The focusing force is zero inside the channel for a very relativistic particle. The spikes at the channel walls are

positron-beam driven

LETTER

doi:10.1038/nature14890

**Multi-gigaelectronvolt acceleration of positrons
in a self-loaded plasma wakefield**

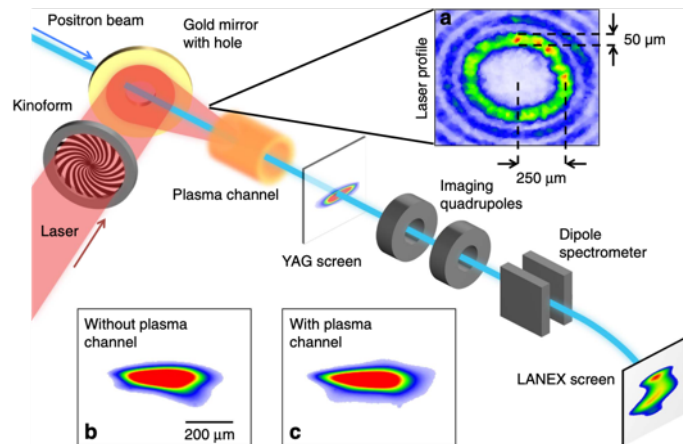
S. Corde^{1,2}, E. Adli^{1,3}, J. M. Allen¹, W. An^{4,5}, C. I. Clarke¹, C. E. Clayton⁴, J. P. Delahaye¹, J. Frederico¹, S. Gessner¹, S. Z. Green¹, M. J. Hogan¹, C. Joshi⁴, N. Lipkowitz¹, M. Litos¹, W. Lu⁶, K. A. Marsh⁴, W. B. Mori^{4,5}, M. Schmeltz¹, N. Vafaei-Najafabadi⁴, D. Walz¹, V. Yakimenko¹ & G. Yocky¹

vents positron acceleration. To avoid this problem, the use of a hollow plasma channel to produce wakes without a focusing force^{13–15}, or the



ARTICLE

Received 17 Nov 2015 | Accepted 27 Apr 2016 | Published 2 Jun 2016



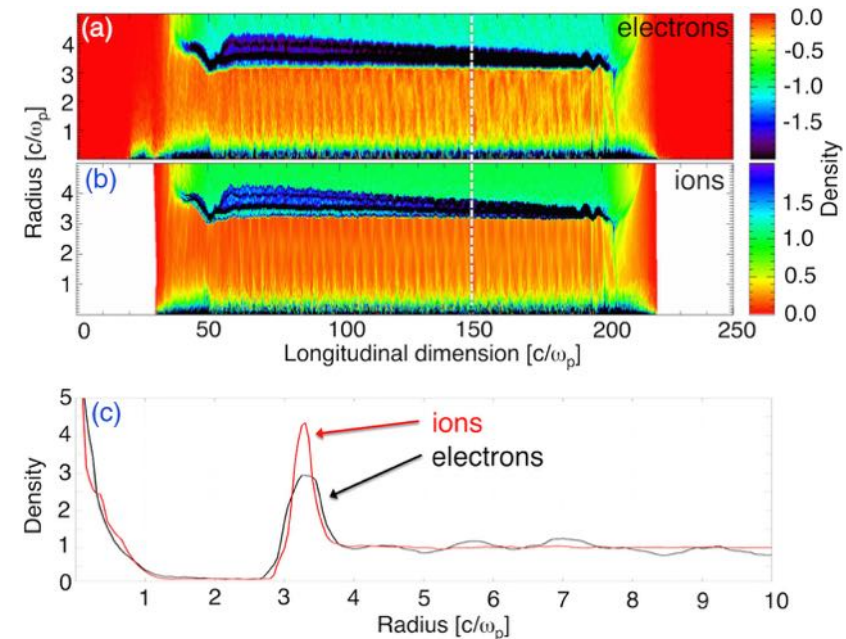
un-ionized gas within the channel

PHYSICAL REVIEW ACCELERATORS AND BEAMS **20**, 081004 (2017)

Excitation of a nonlinear plasma ion wake by intense energy sources with applications to the crunch-in regime

Aakash A. Sahai*

Department of Physics, Blakett Laboratory and John Adams Institute for Accelerator Sciences, Imperial College London, London, SW7 2AZ, United Kingdom, and Department of Electrical Engineering, Duke University, Durham, North Carolina 27708, USA
(Received 5 February 2017; published 23 August 2017)





University of Colorado
Denver

Hollow-channel – first expt.s



e⁺-beam -driven

$$r_{ch} = 16 c/\omega_{pe}$$

$$n_b = 1.3 n_0$$

$$\sigma_z = 1.5 c/\omega_{pe}$$

$$\sigma_r = 0.3 c/\omega_{pe}$$

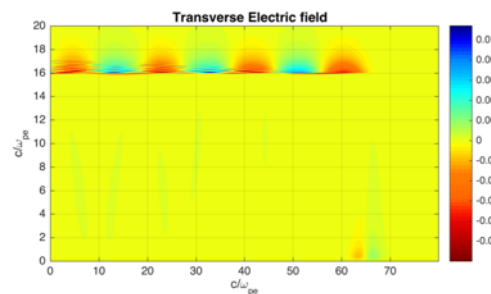
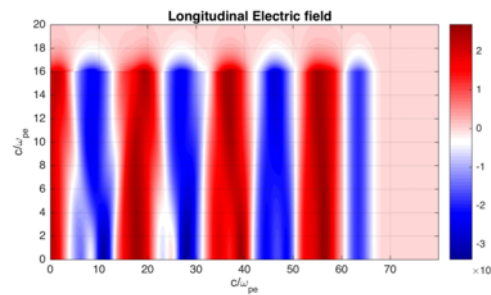
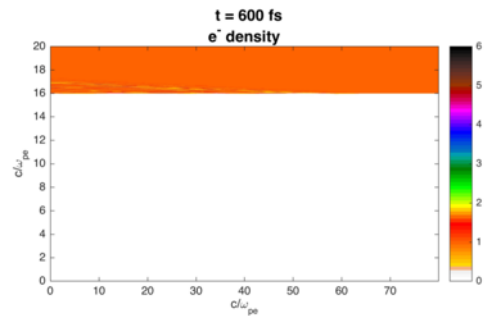
$$\gamma_b = 1000$$

NO focusing forces

currents in the wall

EM acc. fields leak
into the channel

$$10^{-2} E_{WB}$$



CYL
geometry



ARTICLE

Received 17 Nov 2015 | Accepted 27 Apr 2016 | Published 2 Jun 2016

$$n_0 = 8 \times 10^{16} \text{ cm}^{-3}$$

$$\text{obs. field} = 220 \text{ MV/m}$$

$$\text{WB field} \sim 20 \text{ GV/m}$$

e⁻-beam lin. regime - Hollow-channel



e⁻-beam -driven

$$r_{ch} = 16 c/\omega_{pe}$$

$$n_b = 1.5 n_0$$

$$\sigma_z = 1.5 c/\omega_{pe}$$

$$\sigma_r = 0.5 c/\omega_{pe}$$

$$\Upsilon_b = 1000$$

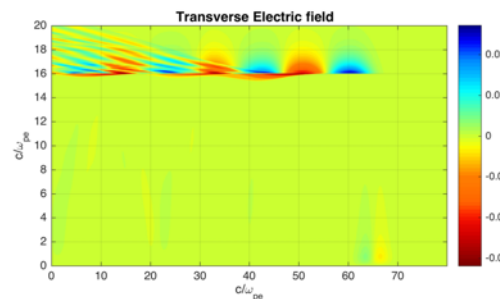
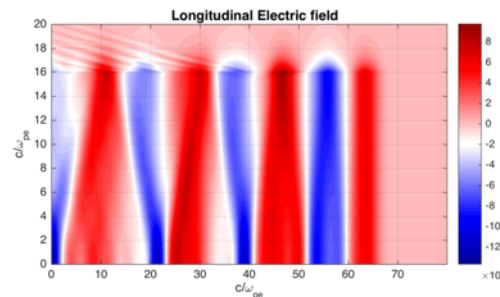
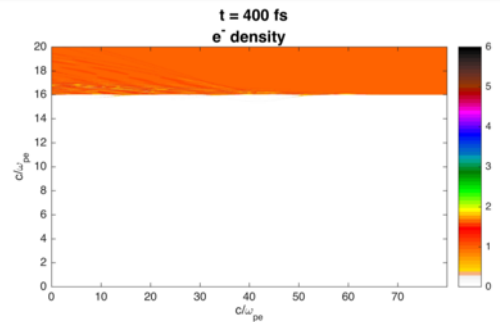
NO focusing forces

currents in the wall

EM acc. fields leak into the channel

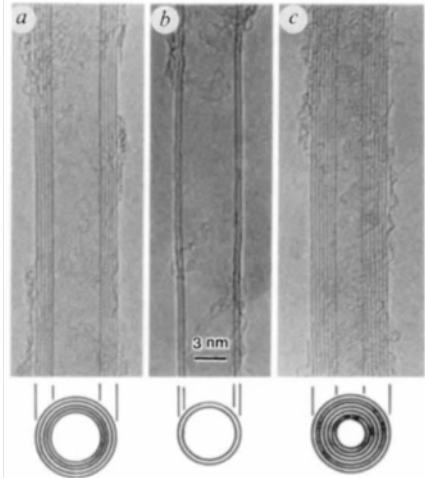
10⁻² E_{WB}

CYL
geometry



- pure EM mode (within channel) - **TM** mode
- not utilizing plasma space-charge electro-static mode
- just like metallic wall waveguide
- weak acceleration fields

Nano-tubes – hollow crystal channels



LETTERS TO NATURE

Helical microtubules of graphitic carbon

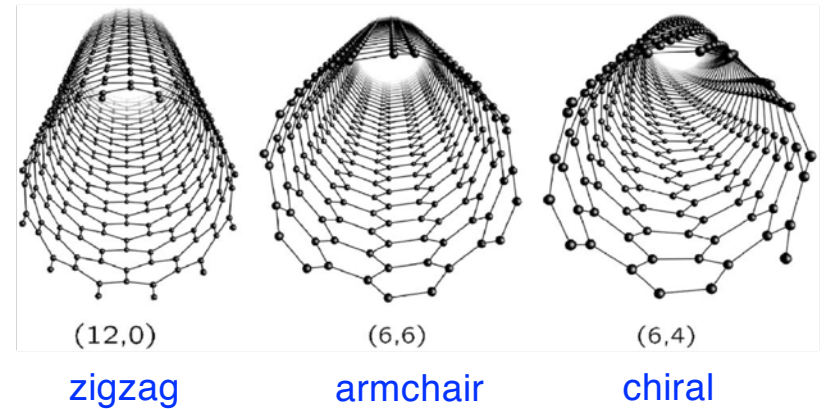
Sumio Iijima

NEC Corporation, Fundamental Research Laboratories,
 34 Miyukigaoka, Tsukuba, Ibaraki 305, Japan

NATURE · VOL 354 · 7 NOVEMBER 1991

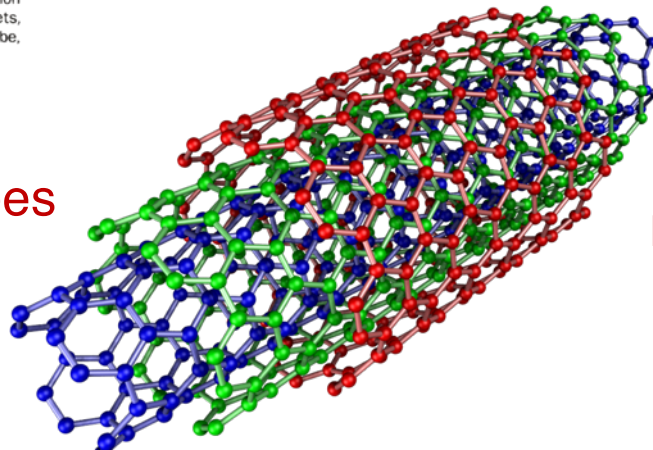
FIG. 1 Electron micrographs of microtubules of graphitic carbon. Parallel dark lines correspond to the (002) lattice images of graphite. A cross-section of each tubule is illustrated. *a*, Tube consisting of five graphitic sheets, diameter 6.7 nm. *b*, Two-sheet tube, diameter 5.5 nm. *c*, Seven-sheet tube, diameter 6.5 nm, which has the smallest hollow diameter (2.2 nm).

single-walled nanotubes (SWNT)



SWNT diameter – 0.3nm to 4nm

multi-walled nanotubes (MWNT)



MWNT diameter – 1.5nm to 100nm

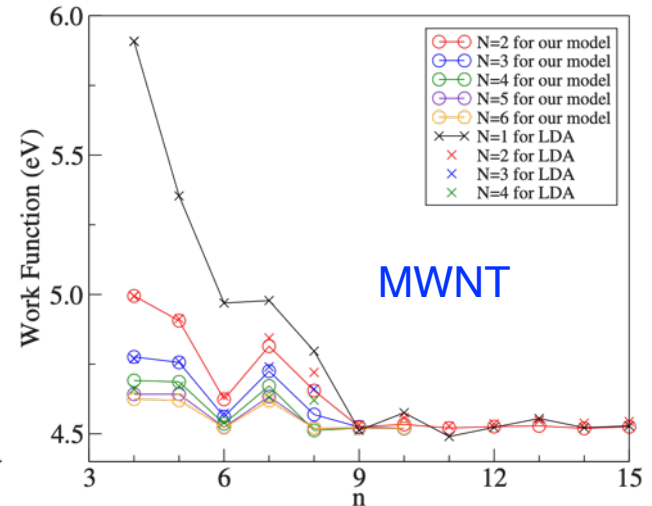
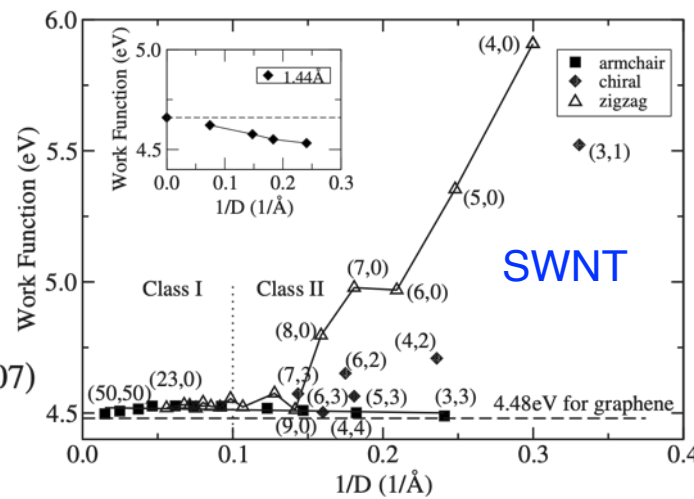
Nano-tubes – properties



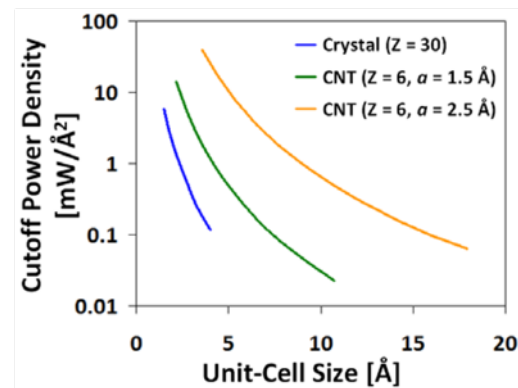
density $\sim 10^{21} - 10^{22} \text{ cm}^{-3}$ $\lambda_{\text{mfp}} \simeq \mu \text{ m}$ collision-less plasma over few ten fs

work function $\sim 5\text{eV}$

PHYSICAL REVIEW B **76**, 235413 (2007)



damage threshold



solid-state modes - plasmonics



simplified wave equation in a dielectric

$$\mathbf{K}(\mathbf{K} \cdot \mathbf{E}) - K^2 \mathbf{E} = -\varepsilon(\mathbf{K}, \omega) \frac{\omega^2}{c^2} \mathbf{E}$$

$$K^2 = \varepsilon(\mathbf{K}, \omega) \frac{\omega^2}{c^2} \quad \text{purely transverse} \quad \mathbf{K} \cdot \mathbf{E} = 0$$

$$\varepsilon(\mathbf{K}, \omega) = 0 \quad \text{purely longitudinal}$$

low-frequency limit – metallic behavior

$$\omega < \omega_p$$

$$\varepsilon(\omega) = 1 - \frac{\omega_p^2}{\omega^2 + i\gamma\omega}$$

high-frequency limit – plasmonic behavior

$$\omega\tau \gg 1 \quad \tau \text{ tens of fs}$$

$$\varepsilon(\omega) = 1 - \frac{\omega_p^2}{\omega^2}$$

bulk plasmon – dispersion $\omega^2 = \omega_p^2 + \frac{6E_F K^2}{5m}$ electron time-scale dominated

bulk phonon – dispersion $\varepsilon(k, \omega) = 1 - \frac{\omega_{pi}^2}{\omega^2 - \omega_{TO}^2} - \frac{\omega_{pe}^2}{\omega^2 - k_x^2 v_e^2}$ ion time-scale dominated

surface plasmon polariton



propagating SPP mode

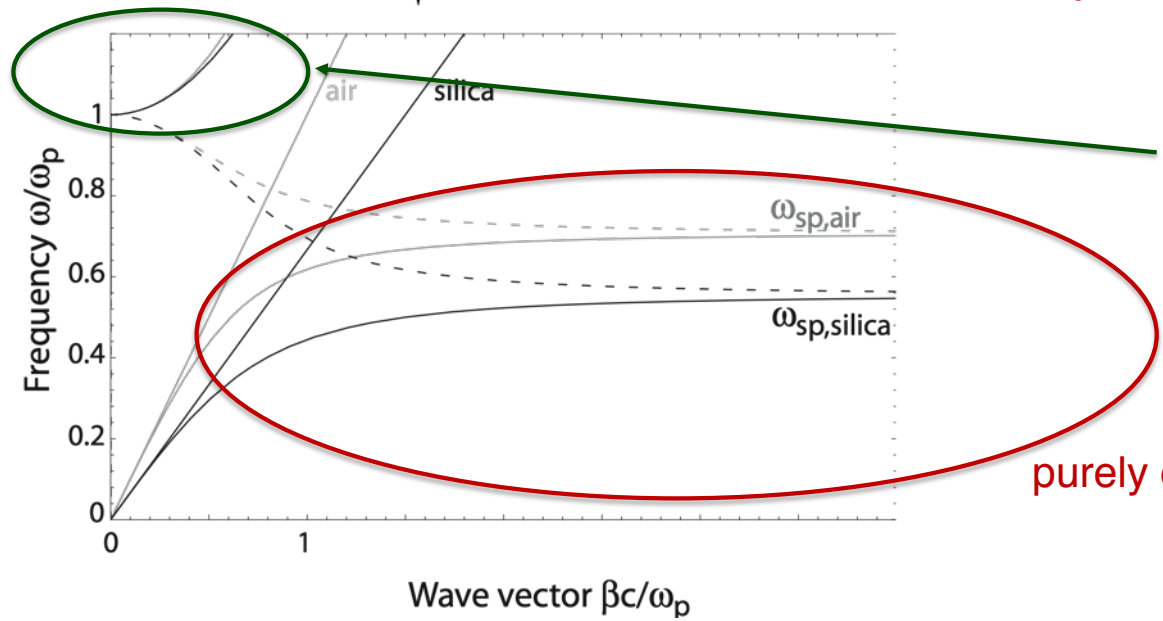
TM-mode existence condition – dispersion relation

surface plasmon frequency

$$\beta = k_0 \sqrt{\frac{\epsilon_1 \epsilon_2}{\epsilon_1 + \epsilon_2}}$$

$$\omega_{sp} = \frac{\omega_p}{\sqrt{1 + \epsilon_2}}$$

also holds for cylindrical geometry



surface plasmon polariton

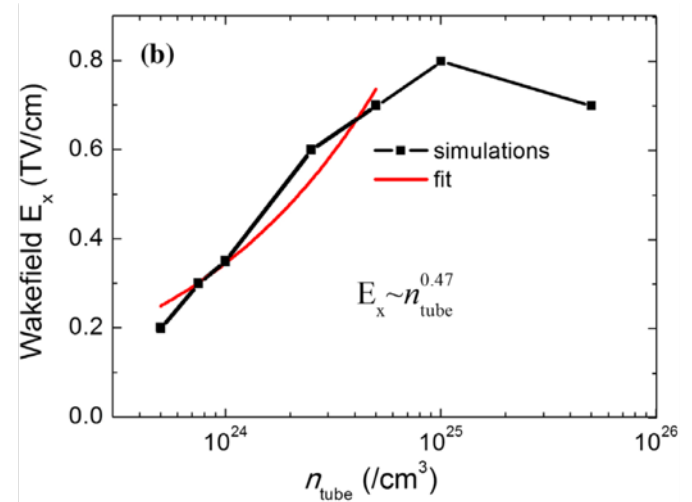
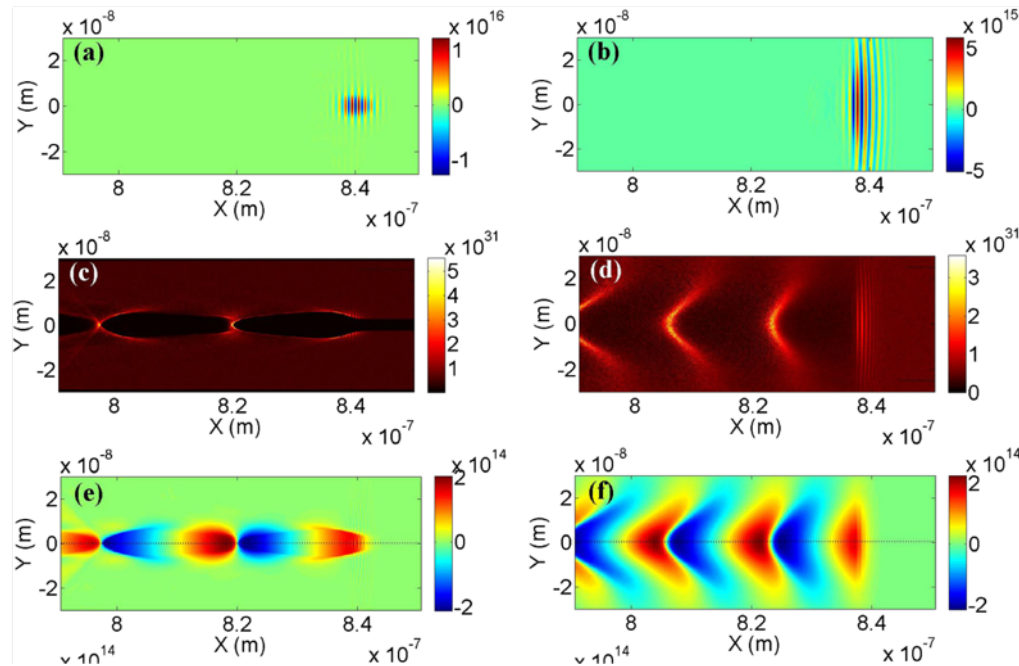
purely electrostatic modes: surface plasmon

Particle-in-cell simulation of x-ray wakefield acceleration and betatron radiation in nanotubes

Xiaomei Zhang,^{1,2} Toshiki Tajima,² Deano Farinella,² Youngmin Shin,³ Gerard Mourou,⁴ Jonathan Wheeler,⁴ Peter Taborek,² Pisin Chen,⁵ Franklin Dollar,² and Baifei Shen¹

TABLE I. Summary of the laser and plasma parameters for our base case.

Laser wavelength λ_L	Peak amplitude a_0	Width radius σ_L	Length radius σ_x	Plasma density n_{tube}	Tube radius σ_{tube}
1 nm	4	5 nm	3 nm	5×10^{24} W/cm ³	2.5 nm/0 nm
1 μm	4	5 μm	3 μm	5×10^{18} W/cm ³	2.5 μm /0 μm



beam-driven Crunch-in regime model

single e⁻ model
kinetic approach

$$m_e \frac{d^2 r}{d\xi^2} + \frac{1}{c^2 \beta_b^2} \frac{n_p e^2}{\epsilon_0} \cdot \frac{1}{2r} (r^2 - r_{ch}^2) = 0$$

Weakly driven
(Linear regime)

$$r^2 - r_{ch}^2 = \cancel{(r - r_{ch})^2} + 2r_{ch}(r - r_{ch})$$

$$\approx 2r_{ch}(r - r_{ch}),$$

$$\frac{d^2 r}{d\xi^2} = -\frac{(\omega_p/c)^2}{\beta_b^2} (r - r_{ch})$$

$$r(\xi) = r_{ch} + A \sin\left(\frac{\omega_p}{c\beta_b} \xi\right)$$

SINUSOIDAL in the weak limit !

Crunch-in regime model - 2



single e⁻ model
kinetic approach

$$r \sim r_{ch}$$

$$\frac{d^2 \rho}{d\xi^2} + \frac{1}{2\beta_b^2} \left(\frac{\omega_p}{c}\right)^2 \cdot \frac{1}{\rho} (\rho^2 - 1) = 0$$

$$\rho = r/r_{ch}$$

autonomous ODE

$$\frac{d}{d\xi} \left[\frac{1}{2} \left(\frac{d\rho}{d\xi} \right)^2 \right] = \frac{d\rho}{d\xi} \frac{d^2 \rho}{d\xi^2}$$

$$\frac{1}{2} \rho'^2 + \frac{1}{2\beta_b^2} \left(\frac{\omega_p}{c}\right)^2 \cdot \left(\frac{1}{2} \rho^2 - \ln \rho \right) = C_1 \quad \rho' = d\rho/d\xi$$

initial condition

$$\rho'_0 \approx \frac{\omega_{pb}}{c} \cdot \frac{1}{\beta_b r_{ch}^{3/2}} \cdot \sqrt{\frac{\sigma_r^2 \sigma_z}{\sqrt{2\pi}}}$$

$$C_1 = \rho'_0{}^2 + \frac{1}{2\beta_b^2} \left(\frac{\omega_p}{c}\right)^2$$

Crunch-in regime model - 3



initial condition

$$\rho'_0 \approx \frac{\omega_{pb}}{c} \cdot \frac{1}{\beta_b r_{ch}^{3/2}} \cdot \sqrt{\frac{\sigma_r^2 \sigma_z}{\sqrt{2\pi}}}$$

**Linear regime
condition**

$$\frac{e}{m_e c \omega_{pe}} \frac{en_b}{r_{ch}^2} \left(\frac{\pi}{2}\right)^{3/2} \sigma_r^2 \sigma_z \ll 1$$

**Crunch-in regime
condition**

$$R_N \simeq \frac{n_b}{n_e} \frac{\sigma_r}{c/\omega_{pe}} \sqrt{\frac{\sigma_z}{c/\omega_{pe}}} \frac{1}{2\sqrt{2}} \left(\frac{\pi}{2}\right)^{1/4}$$

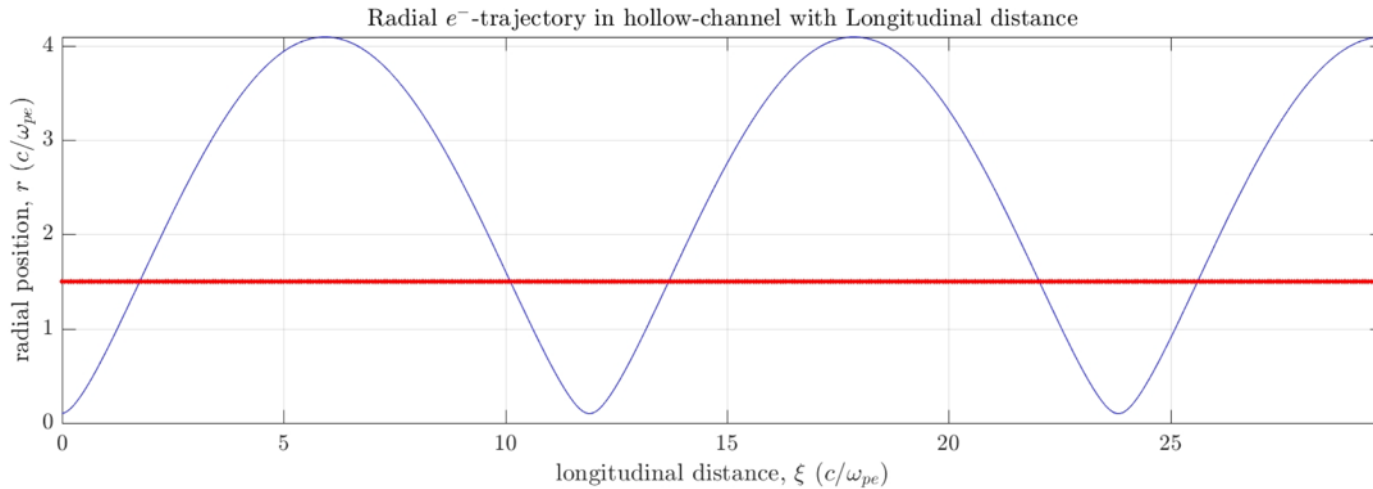
$$R_N = r_{ch} (c/\omega_{pe})^{-1}$$

Crunch-in regime model - 4

single e^- model
 kinetic approach

$$\frac{d^2 \rho}{d\xi^2} + \frac{1}{2\beta_b^2} \left(\frac{\omega_p}{c}\right)^2 \cdot \frac{1}{\rho} (\rho^2 - 1) = 0$$

numerical solution \rightarrow qualitative **Crunch-in** behavior



e⁺-beam driven Hollow-channel

Coherent on-axis compression of e⁻ rings – Crunch-in



$$r_{ch} = 0.6 c/\omega_{pe}$$

$$n_b = 1.3 n_0$$

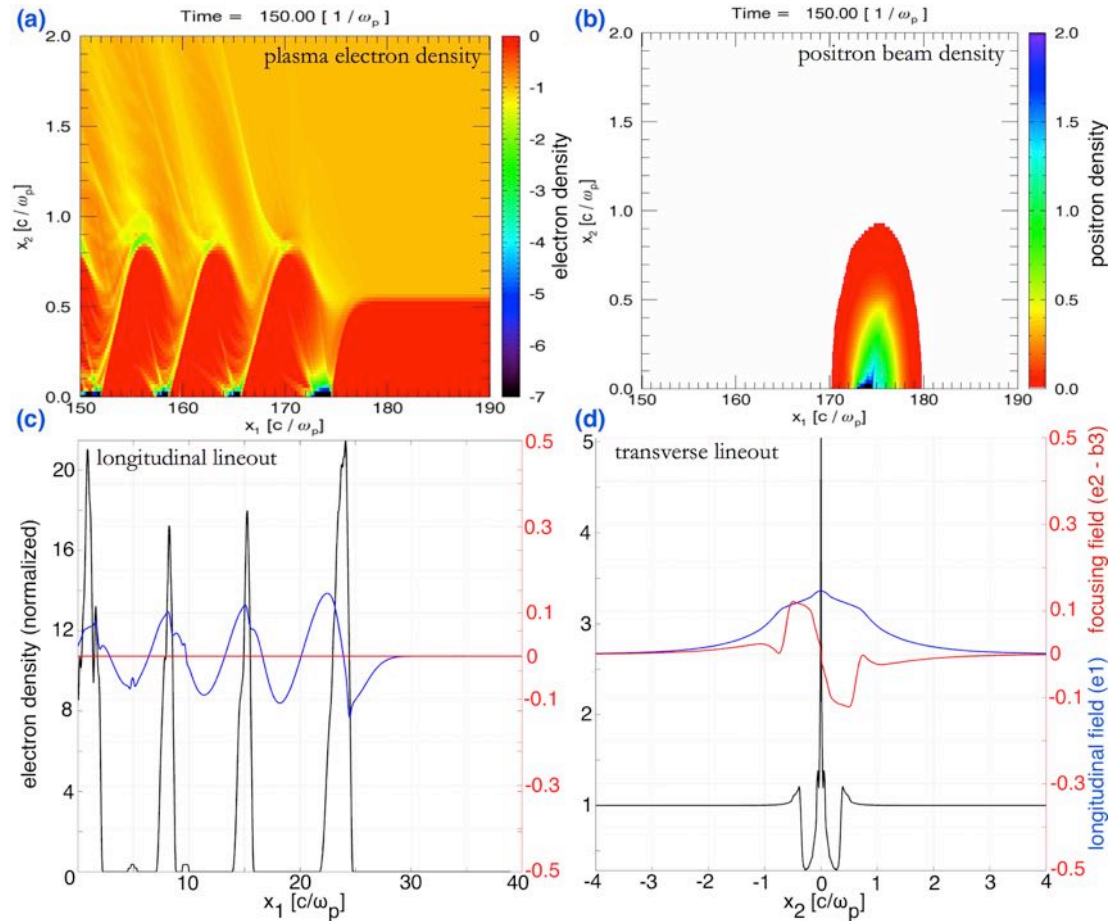
$$\sigma_z = 1.5 c/\omega_{pe}$$

$$\sigma_r = 0.3 c/\omega_{pe}$$

$$\gamma_b = 10000$$

on-axis dynamics

electron density
 transverse field
 longitudinal field



CYL geometry

electron-beam driven “Crunch-in”



matched

$$r_{ch} = 1 \text{ c}/\omega_{pe}$$

$$n_b = 1.5 n_0$$

$$\sigma_z = 1.5 \text{ c}/\omega_{pe}$$

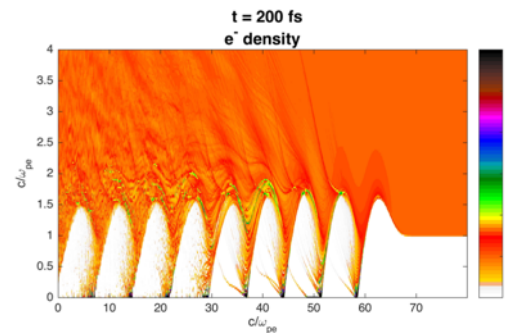
$$\sigma_r = 0.5 \text{ c}/\omega_{pe}$$

$$\gamma_b = 1000$$

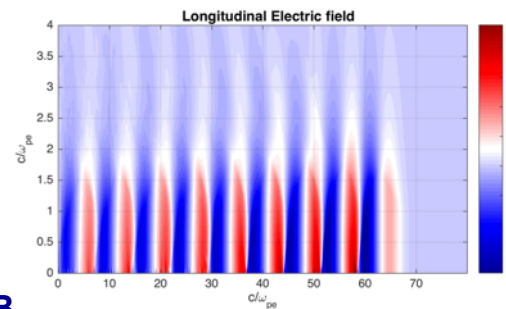
coherent radial oscillations
 e^- collapse to the channel axis

Coherent acc. fields $\sim 0.4 E_{WB}$

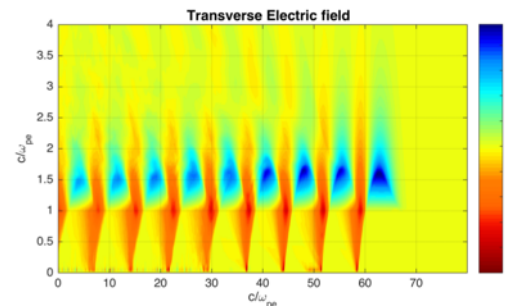
Focusing fields for positrons
 Collocated with acc. fields
 $\sim 0.4 E_{WB}$



CYL
 geometry



WB fields
 accln.
 fields



focusing
 fields for
 positrons

matching collapse-time - channel radius



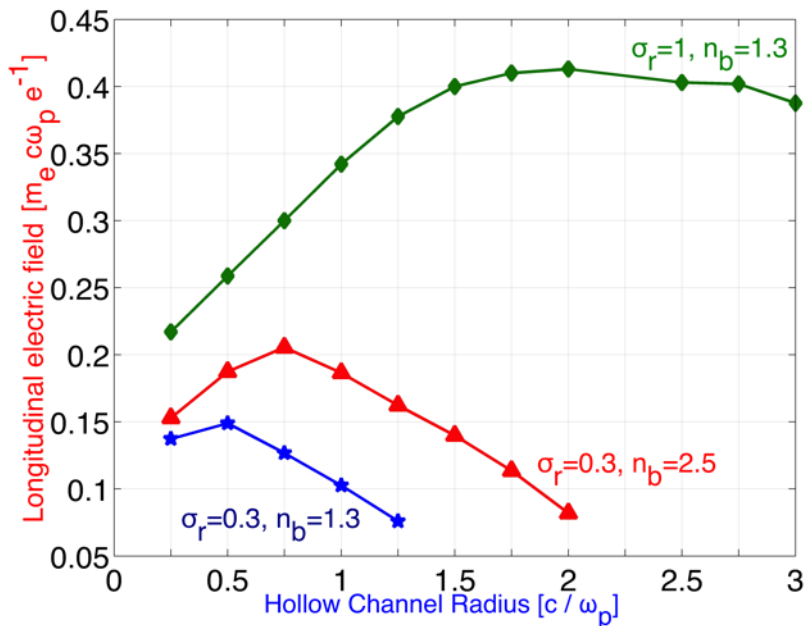
matching collapse time to
“crunch-in” wavelength

$$\tau_c \approx \mathcal{D} \lambda_{Np} / c$$

$$\text{duty-cycle } \mathcal{D} = \frac{\tau_{back}}{\tau_{back} + \tau_{cav}}$$

$$r_{ch}^{opt} \approx 2 \sqrt{\pi} \mathcal{D} \frac{\lambda_{Np}}{\lambda_{pe}} \frac{\omega_{pb}}{\omega_{pe}} r_{pb}$$

**HIGHEST
longitudinal
fields**



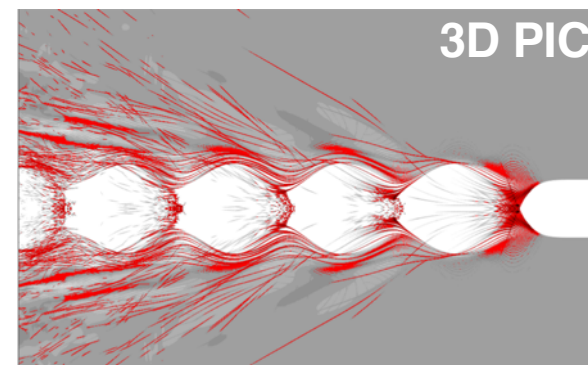
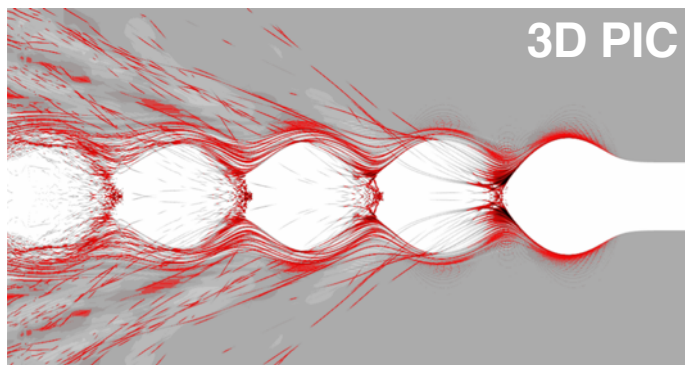
$E_{WB} (n_0 \sim 10^{22} \text{ cm}^{-3}) \sim [\text{few}] \text{ TVm}^{-1}$

$c/\omega_p \sim 100\text{s of nm}$

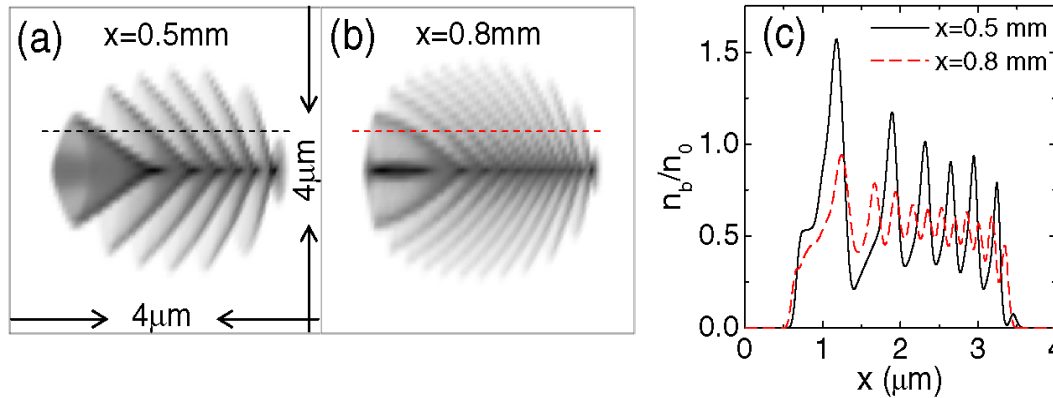
Summary & Ongoing work



1. Proof provided – *existence of the crunch-in regime* – Analysis & PIC-based
2. **decoupled** long. (WB) & tran. fields \rightarrow e^- acceleration
3. **ZERO** defocusing but **focusing** tran. fields \rightarrow e^+ acc.
4. Further investigating – positron / electron **beam-loading** in “crunch-in” regime
5. Further investigating – effect of loss of energy to the wakefields upon the driving energy-sources (**head erosion / etching** etc.)
6. Further investigating – evolution of beam guiding in hollow-channel plasma



beam micro-bunching – beam-plasma interactions



500 MeV

$$n_e = 2n_b \approx 4.4 \times 10^{19} \text{ cm}^{-3}$$

beam betatron
frequency

$$\Omega_b = \omega_{pe} / \sqrt{2\gamma}$$

beam spot-size
oscillation solution

$$\sigma_T(x, \xi) = \sigma_T(0, \xi) | \cos[\Omega_{b0}(1 + \xi/\sigma'_L)x/c] |.$$

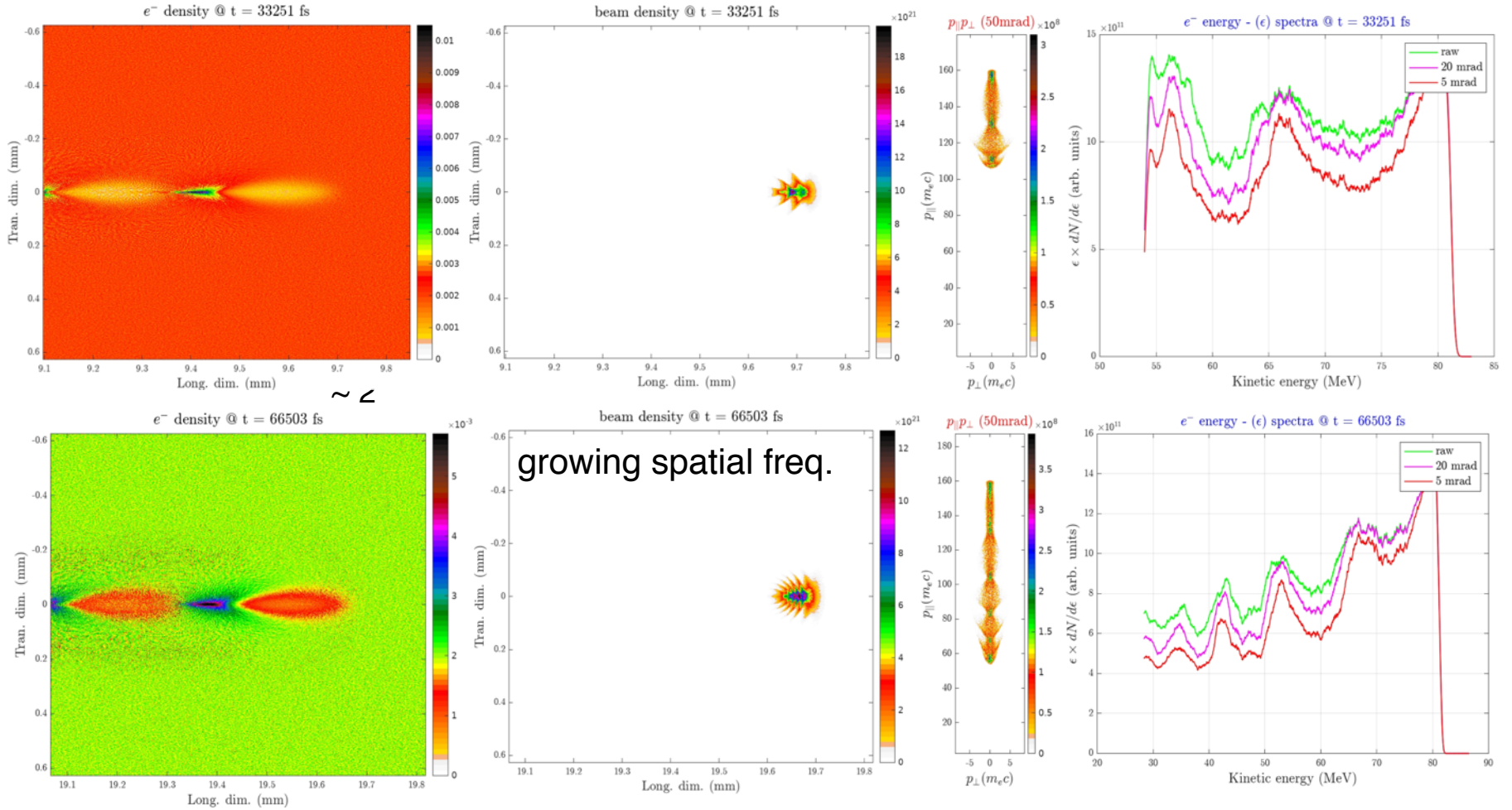
beam spot-size
modulation period

$$\eta = \frac{\pi c \sigma'_L}{\Omega_{b0} x} = \sqrt{\frac{\gamma}{2}} \frac{\sigma'_L}{x} \lambda_{pe},$$



University of Colorado
Denver

bunch-length – $\sigma_r = 50 \text{ } \mu\text{m}$, $\sigma_z/c = 100 \text{ fs}$, $Q = 100 \text{ pC}$, $n_0 = 1 \text{e}16 \text{ cm}^{-3}$

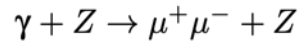


Quasimonoenergetic laser plasma positron accelerator using particle-shower plasma-wave interactions

Aakash A. Sahai*

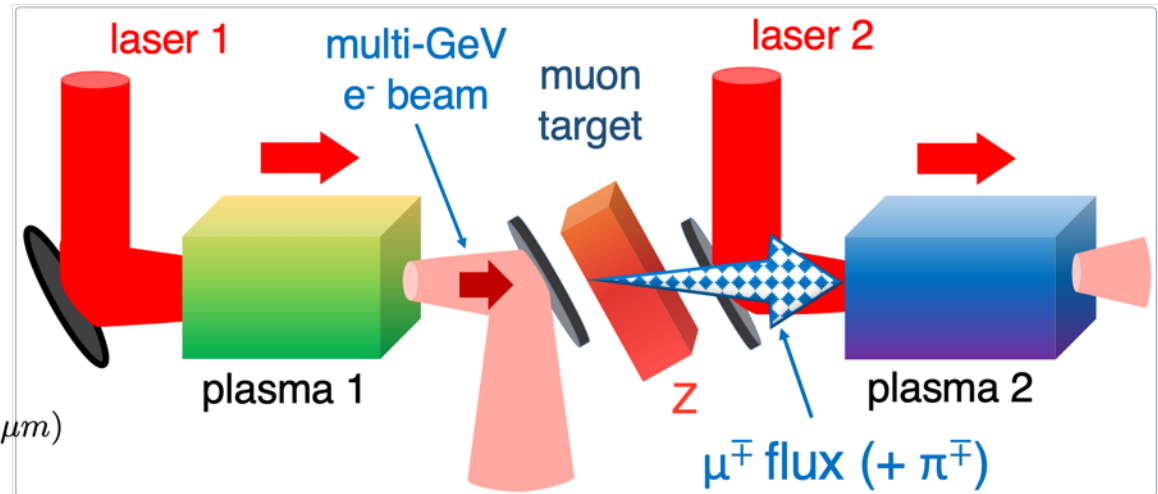
Department of Physics and John Adams Institute for Accelerator Science, Blackett Laboratory,
Imperial College London, SW7 2AZ, United Kingdom

(R.2) Bethe-Heitler muon pair-production reaction:



$$\sigma_{\gamma Z_1 \rightarrow \mu^+ \mu^- Z_2} \simeq \frac{28}{9} Z^2 \alpha r_0^\mu{}^2 \left(\ln \frac{2E_\gamma}{m_\mu c^2} - \frac{109}{42} \right)$$

$$\mathcal{R}_{\gamma Z_1 \rightarrow \mu^+ \mu^- Z_2} (\text{in } 50\text{fs}) \simeq 10^5 \text{ pairs (1nC, 50fs, } \sigma_r \sim 20\mu\text{m)}$$



aakash.sahai@gmail.com